

CHAPTER ONE HUNDRED SEVENTY NINE

RIGID BODY MOTION OF A FLOATING BREAKWATER

Robert W. Miller¹ and Derald R. Christensen²

ABSTRACT

Predictions of the dynamic response of a floating breakwater obtained from a frequency domain analysis are compared with full-scale field measurements. Those parameters prominently affecting accurate response predictions are identified and discussed.

I Introduction

A) Overview

While concrete pontoon floating breakwaters have been successfully used under certain conditions to provide wave attenuation, their design has been primarily based upon empirical considerations. It has only been in the last decade that both the analytical tools and the field data have reached a state of refinement and sophistication which enables the reliable construction and calibration of breakwater response models.

This paper presents a simplified mathematical model of breakwater motion response. The model uses a frequency-domain approach to predict the harmonic responses of a breakwater to short-crested seas for five degrees-of-freedom of rigid-body motion. Rigid-body accelerations for three degrees of freedom as predicted by the model were compared with the corresponding full-scale field measurements. An attempt has been made to identify those parameters which most heavily affect the ability of the model to produce accurate results.

The funding for both the field-measurements and model development was provided by the United States Army Corps of Engineers as part of the West Point Prototype Breakwater Test Project. This project and its scope are more fully described in "Ship-Wake Attenuation Tests Of A Prototype Floating Breakwater" (1984) by Nece and Skjelbreia.

II Field Data

The project site and layout of the instruments of interest to this report are depicted in Figure 1. The two pontoons pictured were rigidly bolted together during the period under discussion. The project site was chosen to maximize exposure to wave attack. Measured

-
1. Associate Member, ASCE, Tongass Engineers, Inc., Juneau, Alaska, U.S.A.
 2. Senior Research Associate, Dept. of Civil Engineering, University of Washington, Seattle, Washington, U.S.A.

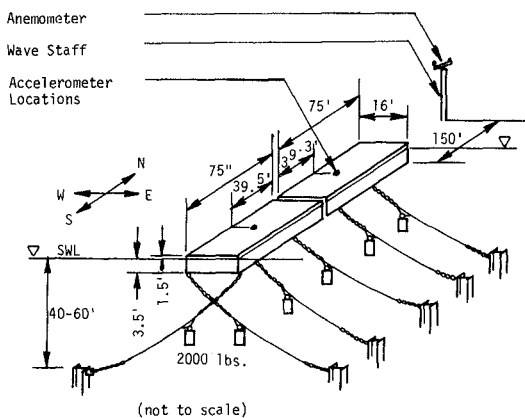


Figure 1. West Point Prototype Floating Breakwater: Project Site Instrument Layout

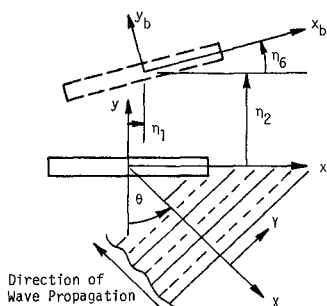


Figure 2. Top View.

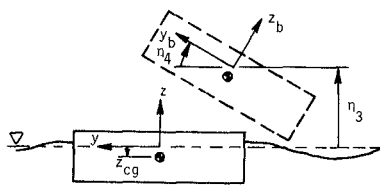


Figure 3. End View.

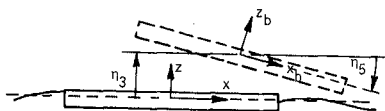


Figure 4. Side View.

Coordinate Definitions

Global: x, y, z
 Equilibrium: x, y, z
 Body: x_b, y_b, z_b

Relative Motion

η_1 = surge η_4 = roll
 η_2 = sway η_5 = pitch
 η_3 = heave η_6 = yaw

quantities which were used in this study were incident wave height, breakwater accelerations, and wind direction. Timeseries of all measured quantities contained 2048 samples (4 samples per second for 8 1/2 minutes).

Incident wave measurements were made at a location 150 feet from the breakwater and located such that wave diffraction or reflection due to the breakwater itself was minimal. Timeseries of incident wave heights were converted into autospectral estimates by means of Fast Fourier Transform techniques. These estimates were used as inputs into the analytical model. Servo-accelerometers measuring sway, heave, and roll were located approximately at the center of mass of each pontoon. Timeseries of these quantities were also transformed and the resulting spectral estimates used for comparison with the model output.

Measurements of wind direction were used to estimate the principal angle of wave attack. This angle was assumed to be coincident with the mean wind direction. The extent to which this assumption is valid is very likely dependent upon the length of time the wind has been blowing in approximately the same direction.

III Description of Model

The analytical techniques employed in breakwater motion prediction are essentially those of ship motion or seakeeping theory as described in St. Denis, 1953; Ochi, 1974; Salveson, 1970. Strip theory is used to estimate the hydrodynamic properties of the body and linear second order differential equations of motion are solved at each discrete frequency of interest. Motion response is therefore confined to the frequency of the excitation with harmonics and second-order effects neglected by the model.

This methodology has been applied to barges (Hutchison, 1977) and breakwaters (Hutchison, 1982; Adey, 1976), but, to the knowledge of the authors, never in a directional sea with the benefit of extensive full-scale data. As pointed out by Hutchison, (1976), barges (and therefore concrete pontoon breakwaters) should be excellent shapes for such an analysis. Many of the problems which have troubled ship motion predictions such as forward speed corrections, bilge keels etc. are absent in breakwaters. Discontinuities in the submerged perimeter are localized in the ends which should provide a suitable situation for strip theory. However, successful treatment of nonlinear phenomenon such as square-law damping or the load-displacement relationships of mooring lines may present additional problems.

B) Coordinates

The coordinate systems used in this analysis are depicted in Figures 2-4. Global coordinates X,Y,Z remain stationary with respect to a fixed point on the earth. The origin of the equilibrium coordinate system is located at the mean still water level in the vertical direction and at the mean position of the center of mass in the horizontal plane. In traditional seakeeping analysis, the

equilibrium frame frequently translates or rotates at a constant rate with respect to the global frame. For a moored breakwater, the distinction between the two frames would only become apparent as a result of long-term changes in mean position of the body due to tide, current, or wind. This distinction, therefore, serves no further purpose in the present analysis.

The body coordinate system (x_b, y_b, z_b) remains fixed in the breakwater itself and is the frame of reference implicitly held by the accelerometers attached to the breakwater.

C) Equations of Motion

The basic equation of motion for the six-degree-of-freedom rigid body response is:

$$\sum_{j=1}^6 (I_{ij} + A_{ij}(\omega)) \ddot{\eta}_j + B_{ij}(\omega) \dot{\eta}_j + (C_{ij} + K_{ij}) \eta_j = F_i e^{i\omega t};$$

for $i = 1$ to 6 3.1

where

- I is the inertia coefficients matrix,
- A is the added mass coefficients matrix,
- B is the hydrodynamic damping coefficients matrix
- C is the hydrostatic restoration coefficients matrix,
- K is the linearized mooring force restoration matrix,
- F is a complex amplitude vector consisting of 6 wave excitation forces,
- ω is the angular frequency of the incident wave,
- η_j is a complex vector describing the amplitude and phase of the motion in the j th direction in the equilibrium frame,
- $e^{i\omega t}$ is a unit vector rotating with angular frequency ω ,

and the dots indicate differentiation with respect to time.

The use of the term "coefficients" is in contrast to "variable" and is not intended to imply non-dimensionality.

The values of the hydrodynamic mass and damping terms as well as the wave excitation forces were determined by the NSRDC Ship Motion and Sea Loads Computer Program (Meyers, 1975), which has exhibited success in the accurate prediction of the motion of destroyer hulls (Salveson, 1970).

Linearized mooring force restoration stiffnesses were obtained from Program BRKMOOR (Adee, 1976) which uses a finite-element approach to establish the equilibrium position of the breakwater. Restoring constants are then determined by perturbing the breakwater from its equilibrium position and calculating the change in mooring tension that

results.

D) Modeling of Square-Law Roll-Damping

The hydrodynamic damping terms presented in the previous section produce damping forces which are linearly proportional to the velocity of the motion. It has been found (Salveson, 1970; Ochi, 1976) in the case of ships that such neglect of higher order (e.g. damping proportional to the square or cube of the velocity) produces satisfactory response prediction except in the case of roll motion. If significant wave energy is present near the roll natural frequency, then the predicted roll response will be much too great. In the case of the West Point floating breakwater, it was also found necessary to include an accounting of square-law roll damping in the analytical model in order to avoid overprediction.

While space limitations preclude a detailed treatment in this report, a thorough development of the following equations may be found in (Schmitke, 1978) for the interested reader. Since a floating breakwater has no mean forward velocity, the only sources of square-law roll damping considered were those due to eddy-making and those due to hull-friction. The approach employed was to calculate the amount of work done by the aforementioned nonlinear damping forces during a complete roll cycle. An equivalent linear roll damping coefficient, B^*44 was then defined which dissipates the same amount of energy during the cycle. Since the amplitude of the roll motion must be known to calculate the energy dissipation, the procedure involved is iterative, requiring repetitive solution of the equations of motion until the calculated and assumed roll amplitudes are in sufficiently close agreement.

Equation 3.1 described above is solved repeatedly at each discrete angle of wave attack and frequency of interest. If the excitation force used is that which would be caused by a wave of unit amplitude incident upon the structure, the solution results in a complex vector termed the frequency response operator or FRO. This quantity is also referred to in the literature as the transfer function. The FRO provides a linear transformation between the amplitude and phase of the wave and that of the motion response of the breakwater. For a particular frequency and angle of wave attack this relationship is:

$$S_{\eta}(\omega, \theta) = H_{\eta}(\omega, \theta) S_{\xi}(\omega, \theta) H_{\eta}^*(\omega, \theta) \quad 3.2$$

where $S_{\eta}(\omega, \theta)$ is the response autospectrum for a given frequency and angle

$S_{\xi}(\omega, \theta)$ is the incident wave height autospectrum for that frequency and angle

and $H_{\eta}(\omega, \theta)$ is the FRO for the frequency ω and angle θ and the superscript * denotes the complex conjugate

Since a random short-crested sea-state may be represented at the summation of monochromatic waves of different frequencies and direction (St. Denis, 1953), it is possible, by means of linear superposition, to

predict the response to a variety of sea states given a complete set of appropriate FROs. This is done using the following form of equation 3.2 given in discrete form:

$$S_{\eta}(\omega) = \int_{-\pi}^{\pi} [H_{\eta}(\omega, \theta) S_{\xi}(\omega, \theta) H_{\eta}^*(\omega, \theta)] d\theta \quad 3.2a$$

Since directional spectra for the project site were not known, it was assumed that

$$\begin{aligned} S_{\xi}(\omega, \theta) &= S_{\xi}(\omega) \Psi(\theta) & 3.3 \\ \int_{-\pi}^{\pi} \Psi(\theta) d\theta &= 1.0 & 3.4 \end{aligned}$$

The form of $\Psi(\theta)$ employed was

$$\begin{aligned} \Psi(\theta) &= K \cos^n(\theta - \theta_0), \quad -\pi/2 \leq \theta \leq \pi/2 & 3.5 \\ \Psi(\theta) &= 0 \quad \text{otherwise} \end{aligned}$$

where $\Psi(\theta)$ is referred to as the spreading function
 θ_0 is the principal or mean angle of wave attack
 and K is a constant chosen to satisfy equation 3.4

F) Operator Transformations

As mentioned previously, solution of the equations of motion in the form in which they have been presented results in displacement frequency response operators about the origin of the x y z coordinate frame. To enable direct comparison of predicted with measured results these operators must i) relate to accelerations, not displacements ii) be valid at the physical location of the instruments and iii) be written in the body rather than equilibrium coordinate system. These transformations will be briefly outlined.

i) Acceleration FRO

since $H_{\eta}(\omega, \theta)$ is assumed to be of the form

$$H_{\eta}(\omega, \theta) = H_{\eta}(\theta) / e^{i\omega t} \quad 3.6$$

it follows that

$$H_{\eta}''(\omega, \theta) = -\omega^2 H_{\eta}(\theta) / e^{i\omega t} \quad 3.7$$

$H_{\eta}''(\omega, \theta)$ is referred to as the Acceleration FRO.

ii) Spatial Transformation

In general if $\{A\}$ and $\{R\}$ are translational and rotational vectors respectively then

$$\{A(x, y, z)\} = \{A_0(x_0, y_0, z_0)\} + \{R_0\} X \{r\} \quad 3.8$$

where the subscript '0' denotes the original (untransformed) location, r is the position vector from (x_0, y_0, z_0) to (x, y, z) and 'X'

denotes the vector cross-product.

iii) Transformation to Body Coordinates

Acceleration in the body coordinate system is defined by the following relation:

$$\{\ddot{A}_b\} = [T] \{A\} \quad 3.9$$

where the subscript 'b' denotes the body coordinate system and [T] is the transformation vector for a sequence of rotation of the Euler angles η_6, η_5, η_4 . For small angles,

$$[T] = \begin{bmatrix} 1 & \eta_6 & \eta_5 \\ \eta_6 & 1 & \eta_4 \\ \eta_5 & \eta_4 & 1 \end{bmatrix}$$

It is to be noted that vectors of rotational quantities are invariant to the foregoing two transformations.

IV Analysis and Discussion

General Method

Many of the parameters required as input into the analytical model just described are not known with certainty. Since one of the purposes of this work was to establish estimates of these values which yielded acceptable response predictions, a consistent method was desired for varying the input parameters. Because much of the processing was done on relatively slow microcomputers, it was necessary to allow flexibility in the application of this method to insure that a reasonable amount of data was examined.

Unknown quantities which appeared to have the largest influence upon the shape and magnitude of the predicted results include the value of the exponent in the cosine-power spreading function, the mooring stiffnesses, the value of the effective bilge radius of the breakwater cross-section, and the reciprocal wave steepness, $1/WS$ which is defined as the wave length divided by the wave height. The latter two quantities primarily influence roll while it is shown later that the mooring stiffness only significantly affect the sway response. The value of 'n' is therefore the only value of large uncertainty which has a substantial influence over the heave response.

Calibration of R_e , the bilge radius, was performed by selecting an input wave spectrum based upon measurement taken during a strong steady wind which blew for several hours directly to beam. A value of n was found which appeared to give good results for heave acceleration response. The values of R_e and the wave steepness were then varied until good results in roll were obtained. While the wave steepness could be expected to change with variations in the wave climate, the bilge radius is a property of the breakwater cross-section and should not change, although its proper value for a cross-section with flat

sides and sharp corners is not obvious. Therefore, after initial calibration, its value was not altered in subsequent runs.

Statistical Measures of Predictive Accuracy

It is appropriate to mention that the spectral density functions derived from measurements are estimates. The 95% confidence band ranges between 0.65 and 1.75 of the plotted ordinate. In most cases, differences between analytical model outputs and spectral estimates fall well within the 95% confidence band. For this reason, conclusions should be drawn based upon trends in the analysis which appear over several runs rather than upon one record only.

In order to present and discuss the results meaningfully for a large number of runs, it was desirable to develop some quantitative measures of closeness of the predicted and measured autospectral estimates. Two quantities were used for this purpose: the predicted variance normalized by the measured variance, henceforth referred to as the variance ratio, VR;

$$VR = \frac{\sigma^2 \text{ predicted}}{\sigma^2 \text{ measured}} \quad \text{where } \sigma^2 \text{ is the response variance} \quad 4.2$$

and the normalized squared error, E_n^2 as defined by the following:

$$E_{n,4.2}^2 = \frac{\epsilon}{\omega} \left[\left\{ \frac{\ddot{S}_n(\omega) \text{ measured}}{\sigma^2 \text{ measured}} - \left(\frac{\ddot{S}_n \text{ pred.}(\omega)}{\sigma^2 \text{ pred.}} \right) \right\}^2 \right]$$

where the summation is over each of the discrete frequencies analyzed.

The variance ratio is intended as an indication of the closeness of the predicted to the measured response magnitudes with 1.0 expressing perfect agreement, numbers greater than 1.0 indicating over-prediction, and numbers less than 1.0 indicating underprediction of the acceleration response magnitude. This statistic, however, does not consider the closeness of the shapes of the curves under comparison, which may differ appreciably while enclosing the same area. When both spectra to be compared to one another are normalized so that each encloses a unit area, the extent to which E_n^2 differs from zero is strictly a result of differences in general shape between the two curves. Identical curves, translated with respect to one another along the frequency axis, however, would have different values of E_n^2 . The unidirectional wind duration, uwd, was defined as the number of hours that the mean wind direction remained within 20 degrees of the mean for the record under consideration.

Evaluation of Results

Table 1 summarizes the results obtained for all model runs made. Overall agreement is generally good except where the wind direction was not steady for several hours or when the significant wave height was low. No obvious overall trends were evident, except perhaps for the

Date 1983	Run#	H _s feet	Wind Angle degrees	Unidir Wind Dur hours	1/WS nd	n nd	HEAVE		ROLL		SWAY	
							VR nd	E _n ² sec ²	VR nd	E _n ² sec ²	VR nd	E _n ² sec ²
4/24	1	2.1	3.5	6	125	9	1.02	4.6	.95	5.7	.90	13.7
4/24	2	1.4	4.2	10	125	*	0.99	7.2	1.03	7.5	1.10	11.4
4/8	3	1.8	16.5	0	125	7	0.56	7.6	0.46	16.84	0.54	5.5
4/8	4	1.6	10.0	8	125	7	1.06	2.6	0.93	15.5	0.87	15.3
4/9	5	1.5	19.0	8	175	18	0.98	5.7	0.98	19.8	0.96	5.9
4/12	6	0.8	24.5	2	400	7	1.21	18.0	0.54	93.9	0.53	58.4
4/13	7	0.6	25.0	0	400	1	1.27	24.8	0.43	101.0	0.47	58.0
4/24	8	1.8	4.3	8	125	18	1.02	21.4	0.89	14.8	0.93	11.1
4/24	9	1.9	8.5	2	125	7	1.04	25.3	1.20	20.2	0.65	74.4
5/28	10	0.9	27.0	6	300	5	0.73	22.1	0.55	63.4	0.47	21.5
4/23	11	1.0	24.2	8	125	9	1.13	97.0	0.85	100.0	0.50	51.2
4/12	12	1.0	3.3	8	175	12	1.00	85.6	0.97	28.8	0.83	11.2
5/6	13	1.0	2.6	8	135	12	1.21	24.1	0.88	41.6	1.02	19.6

* unidirectional wave: n = infinity
 nd = non-dimensional

Table 1 Summary Statistics for all Model Runs (1983)

sway and roll variance ratios to be low rather than high while in heave they tended to be high rather than low. It is encouraging that no degree of freedom experienced inordinately poorer results than the others suggesting a proper balance of terms in the equations of motion. Figure 5 through 7 show typical graphical results obtain for the three degrees of freedom examined.

Heave

In general, more consistent results over a wider range of conditions were obtained for heave than for the other two degrees of freedom, particularly on the records examined which had short wind duration and those with recent wind directional shifts. Even when magnitude discrepancies occurred in heave, the predicted maximum response was at the correct frequency. This is not surprising in view of the fewer uncertain input parameters in heave, the relatively small stiffness provided by mooring restraints in this mode, and the absence of significant higher order damping effects.

Heave acceleration variance ratios ranged approximately from 0.55 to 1.25. The mean variance ratio, averaged over all runs was 1.02 while the normalized squared error, E_n^2 in heave averaged 22.8 over all runs. This value is lower than for the other two degrees of freedom, and if one outlier is discarded, it drops to 16.6.

Roll

The general level of agreement obtained in predicting roll motions is quite good. If only records with fairly constant wind directions for at least four hours are considered, then the ratio of predicted to measured variances ranges from 0.85 to 1.03 with a mean of 0.93. A glance at Table 1 shows that a slight tendency toward underprediction exists overall. If only records are considered during which the breakwater underwent wave attacks within ten degrees of beam, then the mean variance ratio improves to 0.98.

The estimated roll natural frequency is approximately 0.3 hertz which agrees well with both model output and measurements. In runs 6, 7, and 9 the measured peak roll response appears to be shifted slightly toward lower frequencies. Runs 6, 7, and 9 were all of short unidirectional wind duration and records 6 and 7 both exhibit low significant wave heights and relatively large angles of wave attack with respect to beam. Oblique wave attack angles tend to shift the forcing functions to lower frequencies but this should be correctly predicted by the analytical model. Since square law roll damping was only modeled in a narrow frequency range (0.289 to 0.32 hertz) it is difficult to explain a shift of the entire response by means of inaccurate estimation of square law damping parameters.

Sway

Sway is only marginally a harmonic response mode due to the absence of a hydrostatic restoring constant. The mooring restraints do provide

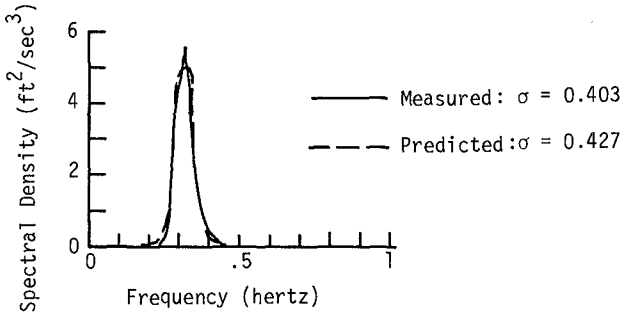


Figure 5. Measured and Predicted Heave Acceleration Autospectral Estimates for West Pontoon: Run 4.

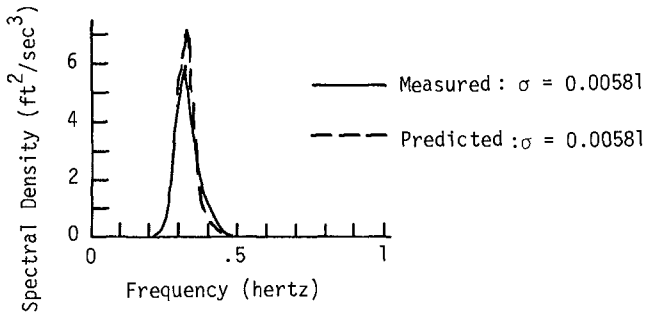


Figure 6. Measured and Predicted Roll Acceleration Autospectral Estimates for West Pontoon: Run 4.

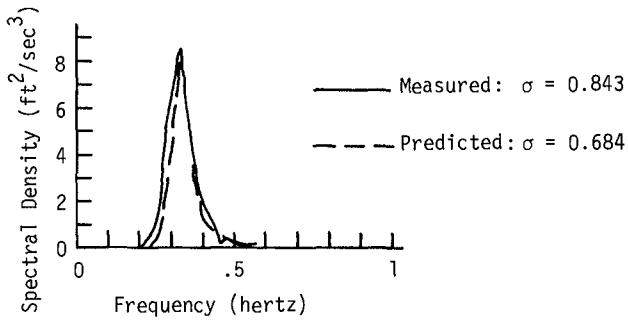


Figure 7. Measured and Predicted Sway Acceleration Autospectral Estimates for West Pontoon: Run 4.

a small restoring force but this does not produce much effect on the acceleration of the body except in the low frequency range. The sway response, however, is harmonic in character due to the periodic nature of the wave excitation force and coupling with other truly harmonic degrees of freedom such as roll. Prediction of sway motions can be difficult because other causes such as wind, tides, and currents can produce significant sways excitations. Long period or steady drift-type forces may have a large effect on mooring stiffnesses which could certainly influence the displacement response and can affect the acceleration response in the low frequency range (Oppenheim, 1980).

It is therefore quite encouraging that the sway variance ratios do not appear to be seriously worse than those of heave or roll. Predicted variance ratios ranged from about 0.5 to 1.1 with a mean of 0.75 over all runs indicating a tendency toward underestimation, particularly as the wind direction veered away from beam. If only records are considered with a mean wind direction within 25 degrees of beam and at least four hours unidirectional wind duration, then the mean variance ratio improves to 0.89. The sway mode was generally more sensitive to input parameters relating to the state of the wave field than either heave or, to a lesser extent, roll.

Although the variance ratios obtained for sway showed poorer agreement than in roll or heave, the mean sway normalized squared error, E_n^2 averaged over all runs was 25.8. This is only slightly higher than for heave (24.5) and significantly lower than roll (40.5). Underestimation of response magnitudes accompanied by good agreement of shape could indicate an underestimation of the forcing functions in the frequency range of maximum wave energy. Such an underestimation would not severely affect the shape of the response curves if it were consistent over attack angles and frequencies of interest, but would cause a depression of the response magnitude.

While these results suggest that a reasonable estimate may be made of the time-varying transverse horizontal inertial force on the body, it should be remembered that some of the considerations mentioned previously would have to be adequately addressed to correctly estimate the lower-frequency forces on the body due to mooring, current etc.

Discussion of Important Parameters

Significant Wave Height

The quantitative measures of closeness, VR and E_n^2 are displayed by significant wave height in figures 8 through 13. A distinction was made between the data records in which the unidirectional wind duration was four hours or greater than those in which it was not.

The accuracy of the heave response predictions shows no particular dependency on H_s while both roll and sway acceleration had noticeably poorer agreement at smaller significant wave heights. There may be a tendency for milder sea states to have a more complex directional character due to higher frequency components in the spectrum. Such

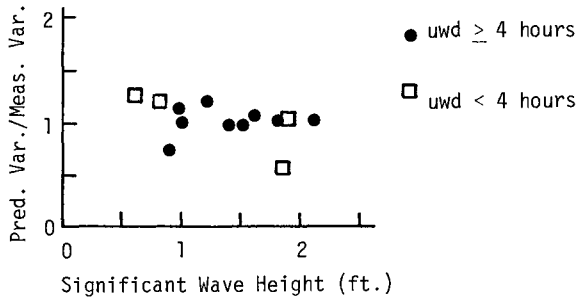


Figure 8. Variance Ratios in Heave Mode versus Significant Wave Height for All Runs.

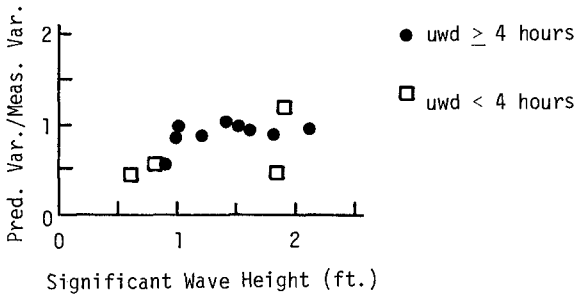


Figure 9. Variance Ratios in Roll Mode versus Significant Wave Height for All Runs.

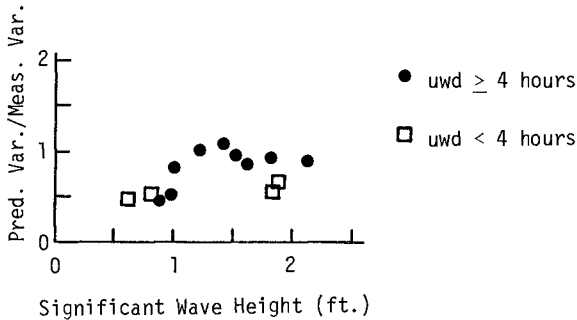


Figure 10. Variance Ratios in Sway Mode versus Significant Wave Height for All Runs.

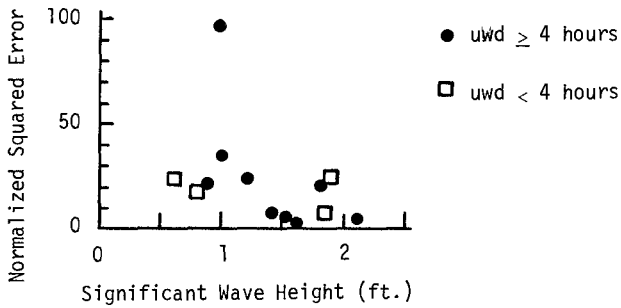


Figure 11. Normalized Squared Error in Heave Mode versus Significant Wave Height for All Runs.

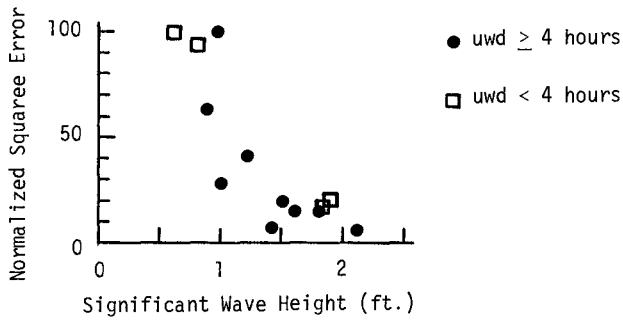


Figure 12. Normal Squared Error in Roll Mode versus Significant Wave Height for All Runs.

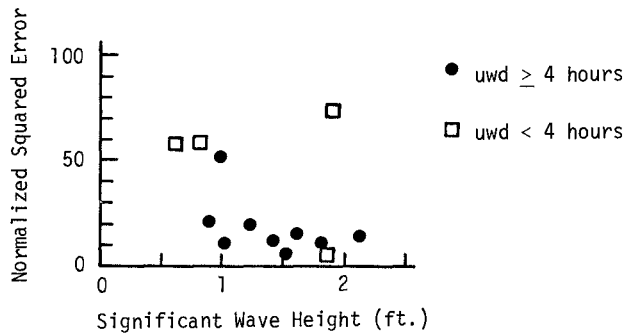


Figure 13. Normalized Squared Error in Sway Mode versus Significant Wave Height for All Runs.

seas would arise and decay faster and respond more quickly to wind shifts. This condition would affect roll and sway more than heave due to the greater sensitivity of these modes to the principal angle of attack. Some of the apparent decline in accuracy, however, is undoubtedly due to the fact that the records with the four smallest significant wave heights all have wind headings of about 25 degrees off beam, so it is unclear which parameter had the greatest effect in reducing agreement.

Wind Direction

Predictive accuracy, as quantified by VR and E_n^2 , was less in the sway and roll modes as the wind direction moved off beam. The data examined only contained wind angles from 0 to 30 degrees off beam, but even this amount of obliqueness appeared to adversely influence the accuracy of the predictions. Since the purpose of a floating breakwater is to provide shelter from incident waves, the ability to accurately predict response to beam seas is of paramount importance, but a lessening of predictive accuracy with such small shifts of the wave attack off beam could indicate a problem with the model. Increments of 10 degrees were used to compute excitation forces, and smaller increments might have been more appropriate.

Directional Spreading Function

The directional characteristics of the limited-fetch short-crested seaway is a subject for which only a very limited amount of data is available. While various methods for modeling this phenomenon exist, the presence of only one node in this analysis made a long-crested superposition approach by far the most straightforward.

Opinions differ as to appropriate values of the exponent, n , in equation 3.5. Generally accepted values range between 2 and 10 for the Puget Sound Region (Langen, 1981).

Some of the values of n found to result in the best agreement between measured and predicted autospectra are higher than can be justified in the literature. Powers of 18 were used twice and on one occasion a unidirectional sea was found to provide the best agreement with the data. The best agreement with the response data was usually obtained when powers of 7 to 12 were employed. It is worthy of mention that values of n which gave the best agreement tended to increase with increasing unidirectional wind duration.

Mooring Forces

The procedure whereby mooring forces are modeled in a frequency domain analysis is a weakness of the method. It is well known that the forces exerted by a non-taut hanging cable are not a linear function of displacement. The question is not so much whether such forces respond linearly to displacements, but over what range of conditions is the error incurred by making such an assumption acceptable.

If second order forces are small and the mooring cables do not lose their hanging catenary shape, the magnitude of the mooring forces are small compared with other forces present such as inertial, wave excitation, and damping. Reasonable estimates of maximum dynamic transverse shear stresses in the major portions of the pontoons themselves could therefore be made despite the rough nature of the mooring force estimates provided by the method of analysis described in this report. Economical design of the mooring system itself, as well as local reinforcement detail in the pontoon near the points of attachment, however, might be better pursued with the aid of a supplementary low-frequency analysis such as described by Oppenheim (1981) or Standing (1981.)

Conclusions

Reasonable agreement was found between acceleration response statistics obtained from a frequency domain model and those based upon measurements from a full-scale floating breakwater. Predicted response variances typically ranged from 0.5 to 1.3 of those obtained from field measurements. Within the limits of the data, predictive accuracy appeared to increase with increasing significant wave height.

The best results were obtained for the heave or vertical degree of freedom. Response magnitudes tended to be underpredicted in many cases in the sway or transverse mode and (to a lesser extent) in the roll of longitudinal rotation modes.

Predictive accuracy appears to be high enough to produce reasonable estimates of the internal forces in the breakwater itself. Caution should be exercised, however, in the sway mode in the low frequency range where slowly varying forces unaccountable by this model may be significant. While the method might therefore be appropriate as a tool in floating breakwater design, other more accurate (and costly) methods may be more appropriate in the prediction of mooring forces.

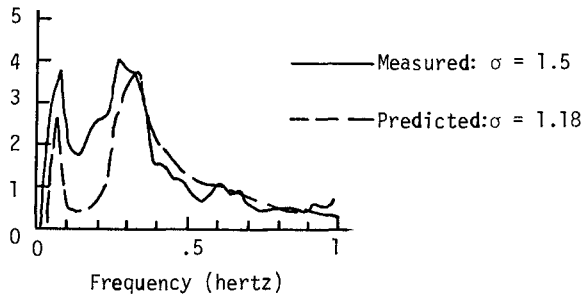


Figure 14. Measured and Predicted Sway Acceleration FRD Moduli for East Pontoon, Run 1: Mooring Stiffnesses from Program BRKMOOR.

References

1. Hutchinson, Bruce L. The Prediction and Analysis of the Motions of Offshore Deck Cargo Barges, MS Thesis, University of Washington, 1977.
2. Hutchinson, Bruce L. "Impulse Response Techniques for Floating Bridges and Breakwaters Subject to Short-Crested Seas," presented at Pacific Northwest Section, Society of Naval Architects and Marine Engineers, 1982.
3. Meyers, W.G. et al, "Manual: NSRDC Ship-Motion and Sea-Load Computer Program," Naval Ship Research and Development Center Report 3376, Washington D.C. February, 1975.
4. Nece, R.E., Skjelbreia, N.K., "Ship-Wake Attenuation Tests Of A Prototype Floating Breakwater", presented at ASCE Conference, Houston, Texas, August, 1984.
5. Ochi, Michel K., "Review of Recent Progress in Theoretical Prediction of Ship Responses to Random Seas," Seakeeping 1953-1973 SNAME T & R Symposium S-3, June 1974, pp. 129-192.
6. Oppenheim, B.W. and Wilson, P.A., Low-Frequency Dynamics of Moored Vessels, Giannotti and Associates, Inc. February, 1980.
7. St. Denis, Manley and Pierson, William J. Jr., "On the Motion of Ships in Confused Seas," Trans. SNAME, Vol. 61, 1953, pp. 280-357
8. Salvesson, N., Tuck, E.O., and Faltinsen, O.M., "Ship Motions and Sea Loads," Trans. SNAME, Vol. 78, 1970, pp. 250-287.
9. Schmitke, Rodney T., "Ship Sway, Roll, and Yaw Motions in Oblique Seas," presented at Annual Meeting, SNAME, New York, N.Y., November 16-18, 1978.
10. Standing, R.G., et al., "Slowly-Varying Second-Order Wave Forces: Theory and Experiment", National Maritime Inst. Feltham England, 1981.